IEEE Access
Multidisciplinary | Rapid Review | Open Access Journal

Received January 12, 2020, accepted January 27, 2020, date of current version February 14, 2020.

Digital Object Identifier 10.1109/ACCESS.2020.2971561

Performance Study of a MIMO Mobile Terminal With Upto 18 Elements Operating in the Sub-6 GHz 5G Band With User Hand

AHMED MOHAMED ELSHIRKASI[1], AZREMI ABDULLAH AL-HADI[1], (Senior Member, IEEE), PING JACK SOH[1], (Senior Member, IEEE), MOHD FAIS MANSOR[2], (Member, IEEE), RIZWAN KHAN[3], XIAOMING CHEN[4], AND PRAYOOT AKKARAEKTHALIN[5], (Member, IEEE)

[1]Advanced Communication Engineering (ACE) Center of Excellence, School of Computer and Communication Engineering, Universiti Malaysia Perlis (UniMAP), Arau 01000, Malaysia
[2]Centre of Advanced Electronic and Communication Engineering, Faculty of Engineering and Built Environment, Universiti Kebangsaan Malaysia (UKM), Bangi 43600, Malaysia
[3]Department of Research and Development, Laird Technologies (M) Sdn Bhd, Perai 13600, Malaysia
[4]School of Information and Telecommunication Engineering, Faculty of Electronic and Information Engineering, Xi'an Jiaotong University, Xi'an 710049, China
[5]Department of Electrical and Computer Engineering, Faculty of Engineering, King Mongkut's University of Technology North Bangkok (KMUTNB), Bangkok 10800, Thailand

Corresponding authors: Azremi Abdullah Al-Hadi (azremi@unimap.edu.my) and Prayoot Akkaraekthalin (prayoot.a@eng.kmutnb.ac.th)

This work was supported in part by the Fundamental Research Grant Scheme (FRGS), Ministry of Education, Malaysia, under Grant FRGS/1/2019/TK04/UNIMAP/02/21, and in part by the Thailand Research Fund through the TRF Senior Research Scholar Program, under Grant RTA 6080008.

ABSTRACT This paper investigates the performance variation when a different number of antenna elements (AEs) is integrated onto a single MIMO mobile terminal, both in free space and when held in a user hand in data mode. Starting with a minimum of two AEs, this investigation assessed the performance of the MIMO terminal with every additional two AEs (up to 18 AEs) in terms of envelope correlation coefficient (ECC), efficiency, multiplexing efficiency, capacity and maximal ratio combining (MRC). The integrated MIMO antennas are identical and operate between 5 and 6 GHz for 5G applications. Results indicated that ECC increased with the number of AEs. However, ECC remains less than 0.32 for the case of 18 AEs in both free space and with a user hand. Meanwhile, the free space efficiency of about 90 % for the two AEs is observed to decrease with the increasing number of AEs to about 50 % with 18 AEs. However, the efficiency of elements changes with user hand depending on the level of interaction between each element and the hand. Direct blockage of AEs by the hand resulted in efficiencies of as low as 5 %, while at the same time, other AEs retained an efficiency of up to 75 %. At the center frequency of 5.5 GHz, the free space capacity is 11.1, 49.5 and 83.2 bit/s/Hz with two, ten and 18 AEs, respectively. However, the use of the mobile terminal in the proximity of the user hand degraded these levels by 11 % (two AEs), 35 % (10 AEs) and 31 % (18 AEs). Finally, multiplexing efficiency showed that capacity degradation is caused mainly by the degradation of AEs efficiency, whereas the impact of low correlation between AEs is found to be an insignificant factor. In addition to the capacity analysis, gain and diversity gain of the maximal ratio combining technique was also investigated.

INDEX TERMS Ergodic capacity, 5G MIMO antenna, mobile terminal, multiplexing efficiency, user effect, maximal ratio combining.

I. INTRODUCTION

Multiple input multiple output (MIMO) antennas have been intensively researched for wireless communication systems for more than two decades due to their capability in achieving high data rates, improving link reliability and immunity against interference without demanding more transmit power or bandwidth [1]–[3]. The elements of MIMO antennas are required to be ideally highly efficiency and lowly correlated within the operating frequency range. Besides that, they should be low cost and strategically installed onto the chassis [4]. Moreover, the MIMO antenna performance also

The associate editor coordinating the review of this manuscript and approving it for publication was Zhen Gao.

depends on the propagation environment and its richness in multipath between the transmitter and receiver [5], [6]. However, the performance of MIMO antennas on user mobile terminal can potentially be restricted when the device is held in different data or talk modes [7]. Using the device in the vicinity of user body causes variation in the radiation pattern of AEs, increases radiated power absorption as well as changes their bandwidth and resonant frequency [8]. Studying the effect of user body on the MIMO antenna of the mobile terminal and proposing some techniques to mitigate this effect is an important research direction in the field of MIMO antenna design for mobile terminals, for example [9]–[14].

Aggregate data rate in 5G wireless communication systems is anticipated to be 1000 times faster than the previous generation, i.e. 4G with more reliability of the wireless link [15]. Thus, MIMO antennas are one of the main factors to enable the achievement of this. Unlike 2G, 3G and 4G systems, in which 2-element and 4-element MIMO antennas have been used in the mobile terminal and are sufficient to fulfill the system requirements, the 5G system needs a higher number of MIMO AEs to achieve the envisioned speed [16]. However, more AEs consume more system resources and increasethe complexity of signal processing. Moreover, the limited space on the user handset restricts the number of AEs that can be placed,and the performance of adjacent AEs degrades with shorter separation distances between them. Thus, the selection of an optimal number of AEs for massive MIMO on the 5G mobile terminal is an important issue to balance the tradeoff between the consumption of available resources and improving system performance. Many sub-6 GHz 5G massive MIMO antennas for mobile terminal have been proposed in the literature. Several instances include an 8-element MIMO antenna for 5G system proposed in [17]–[22], a 10-element MIMO antenna in [23] and [24], a 12-element MIMO antenna in [25] and [26], and a 16-element MIMO antenna in [27]. However, an important aspect absent in these works is the justification in selecting the particular number of elements in each design. Moreover, the performance of these MIMO terminals was studied with a fixed number of AEs, without considering any lower or higher number of AEs as a comparison, and how their increase/reduction will affect the final performance of the MIMO terminal. Finally, the assessments of the use of these MIMO terminals in practice, when held in a user hand, were only discussed in several of these works.

In this work, the performance of 5G MIMO antennas with a varying number of AEs integrated on a mobile terminal is investigated in free space and in the proximity of a user hand. This is aimed at assessing the physical and performance limits of up to 18 identical MIMO antennas integrated within a single mobile terminal chassis and to determine strategies to optimize them. This mobile terminal is studied with different numbers of AEs (M) integrated symmetrically onto its chassis (i.e. 2, 4, 6, 8, 10, 12, 14, 16, 18-elements), and the performance metrics for the MIMO antenna and link metrics are presented. All MIMO antennas are designed to operate throughout the potential 5G frequency band from 5 to 6 GHz, which consists of LTE band 46 ranging from 5150 MHz to 5925 MHz. Although this band is still unlicensed, many MIMO antennas for mobile terminal operating on this band have been proposed and evaluated, for example [8], [26], [28]–[32]. The PIFA topology chosen as the subject of this investigation due to its wide application in mobile terminals. This choice is made with the confidence that the results from this investigation may potentially cater to a wide audience within the scientific community. Finally, the effect of the user hand in this work is investigated when the chassis is held in data mode using a standard hand phantom model compliant to the cellular telecommunication and internet association (CTIA) [33].

This paper is organized as follows. The next section presents the MIMO terminal, antenna design and the initial antenna performance. Section 3 then presents the evaluation metrics, which are derived from discrete radiation pattern data. The results are discussed next in Section 4 prior to the conclusion in Section 5.

II. MIMO ANTENNAS DESIGN

Identical planar inverted-F antennas (PIFAS) have been designed on a chassis using CST microwave studio, as illustrated in Figure 1. These AEs are built using a 0.291 mm-thick copper sheet, and are then located on a Rogers RT/Duroid 5880 substrate dimensioned at 150 × 80 × 1.575 mm^3. Based on the wavelength (λ) at 5 to 6 GHz, the length of the chassis is between 2.50λ and 3.00λ, whereas its width is from 1.33λ to 1.60λ. This substrate features a permittivity, $\varepsilon_{\mathbf{r}} = 2.2$, loss tangent, $\boldsymbol{tan\delta} = 0.0009$. The antenna element is

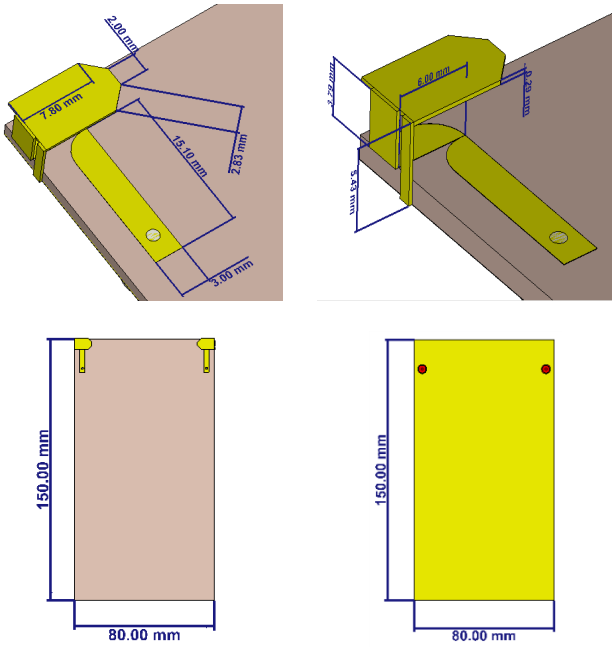

FIGURE 1. Dimensions of AEs and chassis.

also chamfered at the corners to tune the resonant frequency. An L-shaped 50 Ω microstrip feed line printed on the substrate is used to feed this antenna.

Different numbers of AEs are then located onto the chassis, with their distribution for each M from 2 to 18 shown in FIGURE 2. AEs are placed on the outer frame of the chassis symmetrically around the central vertical axis.

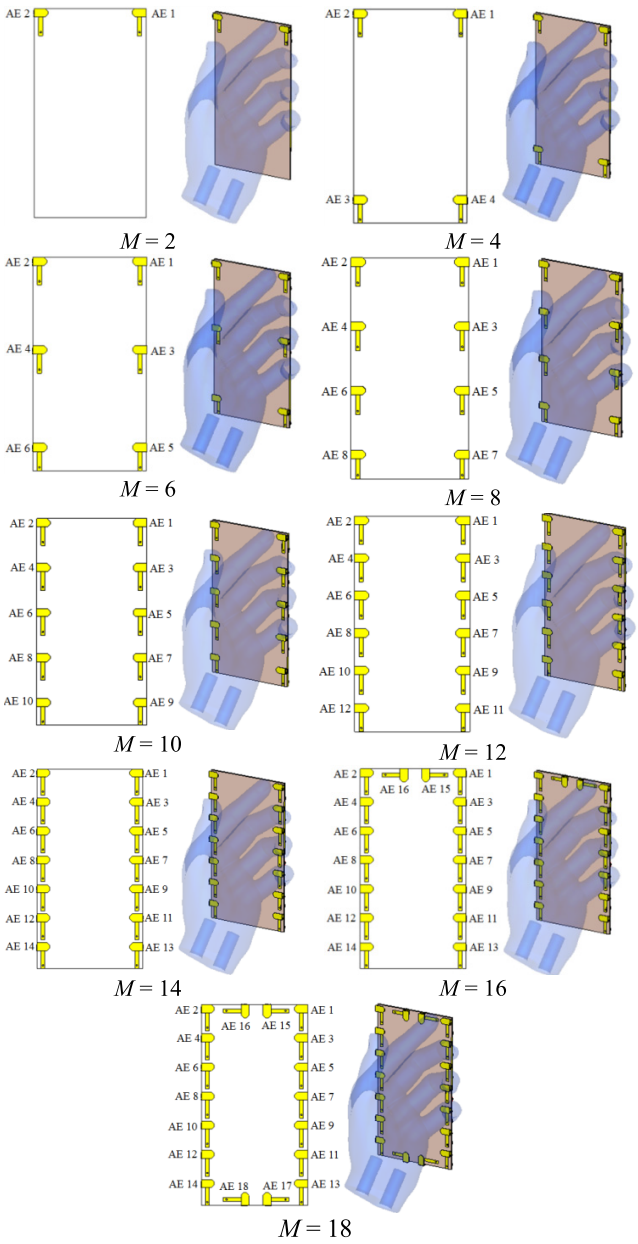

FIGURE 2. Distribution of AEs on the chasses in all values of M and user hand grip.

Besides evaluation in free space, the device is also evaluated when held in a user hand in data mode in terms of S-parameter and radiation patterns. An example of the S-parameters and radiation pattern results for $M = 2$ are shown in Figure 3. It can be observed that $S_{11} = S_{22}$ in free space, and the radiation patterns of AE1 and AE2 are

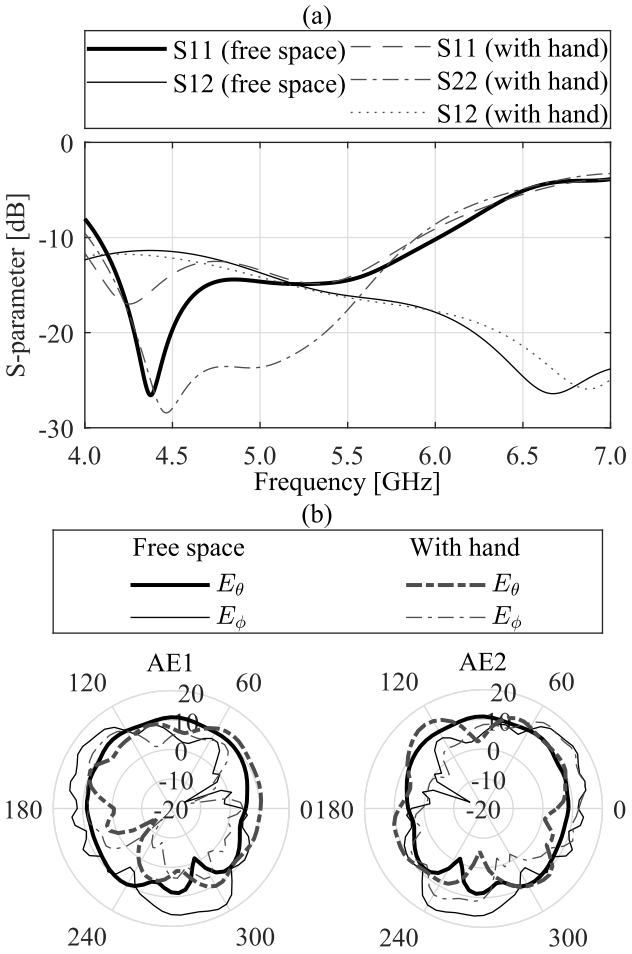

FIGURE 3. S-parameter and radiation pattern of the AEs with $M = 2$ in free space and with a user hand.

symmetrical due to the symmetrical placement of these elements on the chassis. However, the influence of the user hand then made the S-parameters and radiation patterns behaved differently.

III. PERFORMANCE EVALUATION METRICS

This section presents the evaluation metrics that are used to evaluate the MIMO antenna performance in this work. These metrics can be divided into two categories; i) MIMO antenna metrics and ii) MIMO link metrics. Metrics related to MIMO antenna are envelope correlation coefficient (ECC), total efficiency and mean effective gain (MEG). These metrics are used to evaluate other MIMO link metrics. More specifically, ECC and total efficiency are used to build the wireless channel matrix to study the ergodic capacity and multiplexing efficiency. Besides that, ECC and MEG are used in the model of maximal ratio combining (MRC) technique.

A. MIMO ANTENNA PERFORMANCE EVALUATION METRICS

ECC is one of the main performance metrics of MIMO antennas for mobile communications [34]. ECC describes the

correlation (dependence) between every two AEs among all combinations of MIMO AEs. To obtain a satisfactory MIMO antenna performance, ECC should be low so that channels are uncorrelated, and the resulting system has a high diversity and high capacity [35]. The value of 0.5 is widely used in the literature as an acceptable threshold for ECC [36]. However, this value has been revised to 0.3 in 4G wireless communication systems criterion [37]. The ECC ($\rho_{e,jk}$) between AEs i and j can either be calculated using the S-parameter method or from the far-field radiation pattern. However, the S-parameter method is derived based on the assumption of 100% efficient AEs, which is non-existence in practice. Moreover, this method assumes a uniform environment, where the signal incidence is assumed to be equally distributed from all spatial directions. This does not consider other more directive environment models, where the signal may come from certain directions with predefined angular spreads [38]. The far-field radiation pattern method overcomes the above disadvantages, and ECC for this method can be calculated according to [38], (1) as shown at the bottom of this page, where *XPR* is the cross-polarization ratio between vertical and horizontal polarized components, and $E_{\theta i}, E_{\theta j}E_{\phi i}, E_{\phi j}$ are the far-field components of AEs, with the θ and ϕ subscripts denote the vertical and horizontal polarizations, respectively. Parameters P_θ and P_ϕ are the corresponding angular power spectrums (APSs) of the propagation environment which should satisfy the following conditions:

$$\int_0^{2\pi}\int_0^{\pi} P_\theta \cdot \sin(\theta)\, d\theta d\phi = 1,$$
$$\int_0^{2\pi}\int_0^{\pi} P_\phi \cdot \sin(\theta)\, d\theta d\phi = 1 \tag{2}$$

The next parameter is the total efficiency η of an AE, which describes the portion of power radiated out into space in comparison to the total transmitted power. This parameter can be calculated from the far-field radiation pattern of the antenna using the following formula [39]:

$$\eta = \frac{1}{4\pi}\int_0^{2\pi}\int_0^{\pi}\left[E_\theta E_\theta^* + E_\phi E_\phi^*\right] sin(\theta) d\theta d\phi \tag{3}$$

where E_θ and E_ϕ are the radiation pattern fields of the AE in the vertical and horizontal polarizations, respectively.

The next evaluation parameter is the mean effective gain (MEG), which quantifies the ability of the antenna to collect energy from the surrounding environment [33], [39]. MEG is calculated from the far-field radiation pattern according to the following relation [40]:

$$MEG = \int_0^{2\pi}\int_0^{\pi}\left[\frac{XPR}{XPR+1}E_\theta E_\theta^* P_\theta + \frac{1}{XPR+1}E_\phi E_\phi^* P_\phi\right] sin(\theta) d\theta d\phi \tag{4}$$

where E_θ, E_ϕ, P_θ and P_ϕ are the radiation pattern fields of the antenna, and the APS distribution of the incident wave respectively. *XRP* is the cross-polarization ratio.

In case of a uniform environment, the *XPR* value is 0 dB and $P_\theta = P_\phi = 1/4\pi$. Substituting these values in (4) and comparing it with (3) gives [40]:

$$\eta = 2\, MEG \tag{5}$$

The relation in (5) is only valid for uniform APS. For other directive distributions, (3) and (4) should be used separately to calculate η and MEG.

B. MIMO LINK PERFORMANCE EVALUATION METRICS

The proposed wireless channel model in this work is based on the model used in [41]–[45]. This model assumes the same number of antenna elements on both sides of the link, and it focuses on the receiver side with an assumption of an ideal MIMO antenna (i.e. 100 % efficiency of the AEs and zero ECC between the) on the transmit side. Moreover, the channel matrix is constructed using two antenna parameters i.e. efficiency and ECC to show how the MIMO antenna under study affects the capacity and gain of the link. In addition to that, the proposed scenario assumes that the channel state information (CSI) is not known at the transmitter. On the receiver side, the ECC and total efficiency are used to build the correlation matrix, which is used to modify an ideal wireless channel matrix, i.e. an independent and identically distributed (IID) wireless channel matrix. This modification is performed to factor in the non-ideality of the wireless channel in practice, according to the following equation [45]:

$$H = R^{1/2} H_{IID} \tag{6}$$

where R is the correlation matrix and H_{IID} is the IID channel matrix. The correlation matrix R is built as follows

$$R = \Lambda^{1/2}\, \bar{R} \Lambda^{1/2} \tag{7}$$

where Λ is the efficiency diagonal matrix, which diagonal elements are the efficiency of AEs, defined

$$\rho_{e,ij} = \left| \frac{\int_0^{2\pi}\int_0^{\pi}\left(XPR.E_{\theta i}.E_{\theta j}^*.P_\theta + XPR.E_{\phi i}.E_{\phi j}^*.P_\phi\right) sin(\theta) d\theta d\phi}{\sqrt{\prod_{k=i,j}\int_0^{2\pi}\int_0^{\pi}\left(XPR.E_{\theta k}.E_{\theta k}^*.P_\theta + XPR.E_{\phi k}.E_{\phi k}^*.P_\phi\right) sin(\theta) d\theta d\phi}} \right|^2 \tag{1}$$

as follows:

$$\Lambda = \begin{bmatrix} \eta_1 & 0 & \cdots & 0 \\ 0 & \eta_2 & \cdots & 0 \\ \vdots & \vdots & \ddots & \vdots \\ 0 & 0 & \cdots & \eta_M \end{bmatrix} \tag{8}$$

and $\bar{R}$ is the complex envelope correlation matrix defined as [46]:

$$\bar{R} = \begin{bmatrix} 1 & \rho_{c,12} & \cdots & \rho_{c,1M} \\ {\rho_{c,12}}^* & 1 & \cdots & \rho_{c,2M} \\ \vdots & \vdots & \ddots & \vdots \\ {\rho_{c,1M}}^* & {\rho_{c,2M}}^* & \cdots & 1 \end{bmatrix} \tag{9}$$

The complex envelope correlation coefficient $\rho_{c,ij}$ is calculated in a similar way to the ECC in (1) but without the squared absolute value operator.

The ergodic capacity can be calculated after constructing the channel matrix H as follows [38]:

$$c = E\left(log_2\left(det\left(I_M + \frac{SNR}{M} H\,(H)^H\right)\right)\right) \text{ bit/s/Hz} \tag{10}$$

where E is the averaging operator, I_M is the identity matrix of size M, SNR is the signal-to-noise ratio, and M is the number of AEs

The next parameter which describes the channel capacity performance is the multiplexing efficiency η_{mux}. It is defined as the ratio between the signal-to-noise ratio of the IID MIMO system (SNR_{IID}) and the signal-to-noise ratio of the MIMO antenna under test (SNR_{AUT}). Both MIMO antennas at these SNRs have the same ergodic capacity. The value of η_{mux} is then calculated from these linear SNRs as follows [45]:

$$\eta_{mux} = \frac{SNR_{IID}}{SNR_{AUT}} \leq 1 \tag{11}$$

or when these SNRs are on a dB scale:

$$\eta_{mux}\,[dB] = SNR_{IID}\,[dB] - SNR_{AUT}\,[dB] \leq 0 \tag{12}$$

Numerically, η_{mux} can be calculated by selecting a SNR_{IID} value and applying it in (10) with IID channel matrix to find the IID ergodic capacity c_{IID}. The SNR_{AUT} is selected to be $SNR_{IID} + \delta$, where δ is a small amount of signal-to-noise-ratio. This SNR_{AUT} is used in (10) with a channel matrix according to the model in (6) and (7) to calculate AUT ergodic capacit c_{AUT}. Both ergodic capacities i.e. c_{IID} and c_{AUT} are compared, and the process of updating SNR_{AUT} is repeated until both capacities are almost equal within a certain error range. Then η_{mux} is calculated as in (11) using SNR_{IID} and using the most recent value of SNR_{AUT}. However, this approach to find η_{mux} is numerically complicated, and more importantly, it does not provide a direct link between the MIMO antenna parameters, i.e. ECC and efficiency with th η_{mux}. The method which was used in the literature is derived in [45]. This method links η_{mux} with MIMO antenna parameters, i.e. ECC and efficiency as follows:

$$\eta_{mux} = \sqrt[M]{\left(\prod_{i=1}^{M} \eta_i\right) det(\bar{R})} \tag{13}$$

where η_i is the efficiency of i-th AE and $det(\bar{R})$ is the determinant of the complex envelope correlation matrix. Besides its compact form, (13) can be used directly without the need to evaluate ergodic capacity for SNR_{IID} and every updated SNR_{AUT} value. Besides that, this equation relates the antenna parameters directly with η_{mux} in two terms, as follows. The first ter $\sqrt[M]{\left(\prod_{i=1}^{M} \eta_i\right)}$ is the geometrical mean of the individual AEs efficiencies. The second term is $\sqrt[M]{det(\bar{R})}$ which depends on the correlation between AEs. This term approaches 1 when all complex correlation coefficient between AEs are close to 0. Optimizing both terms leads to an improved η_{mux} of the MIMO antenna, and hence achieving a closer level to the IID capacity.

The final MIMO link performance metric is related to the maximal ratio combining (MRC) technique. This technique combines the received signal from MIMO AEs linearly using optimal coefficients [47], [48]. The cumulative distribution function (CDF) of the MRC technique in terms of MIMO antenna parameters, i.e. ECC and MEG is given by [48] as follows:

$$P_{MRC}\,(\gamma \leq x) = 1 - \sum_{j=1}^{M} \frac{\lambda_k^{M-1} e^{-x/\lambda_j}}{\prod_{k \neq j}^{M} (\lambda_j - \lambda_k)} \tag{14}$$

where x is the signal to noise ratio SNR, M is the number of MIMO AEs and λ_j is the eigenvalues of the covariance matrix of size $M \times M$ whose entry $k_{i,j}$ is given by:

$$k_{i,j} = \rho_{e,ij} \sqrt{MEG_i\, MEG_j} \tag{15}$$

where $\rho_{e,ij}$ is the ECC between AEs i and j, MEG_i and MEG_j are the MEG values of AEs i and j.

A summary of the relationships between the performance metrics are shown in Figure 4.

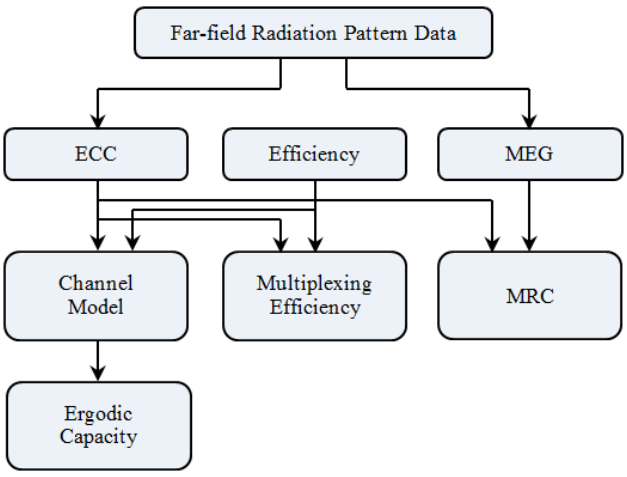

FIGURE 4. Summary of the performance evaluation metrics and the relation between them.

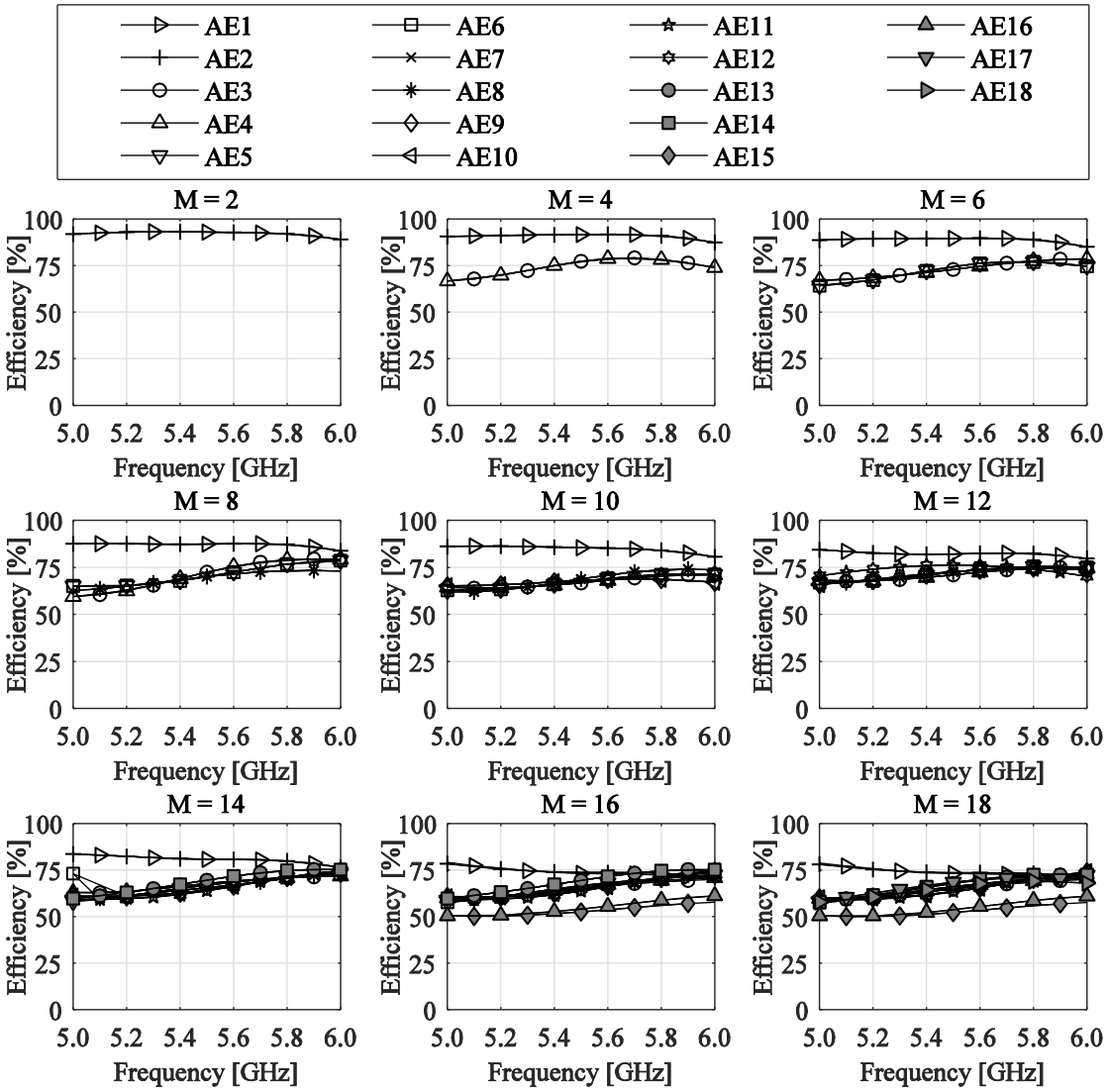

FIGURE 5. The efficiency of each AE in free space with different values of M.

IV. RESULTS AND DISCUSSION

A. ANTENNA PARAMETERS

First, the results of ecc are discussed. The number of ECC values that are evaluated at every simulated frequency point is $\boldsymbol{M(M-1)/2}$. For brevity reasons, the maximum ECC value is selected over the entire frequency range for every increase of two AEs starting from 2 to 18. Both cases of the mobile terminal operating in free space and with a user hand were considered, and their results are presented in Table 1. Results indicated that there is a steady increase in ECC values with M. However, the maximum ECC is 0.32 when M is 18.

Next, the efficiency of the AEs in both cases of free space and with a user hand is studied and presented in Figure 5 and Figure 6, respectively. In free space, the efficiency of AEs changes according to their locations on the chassis and according to the number of AEs. It can be noticed that AE1 and AE2 have the highest efficiency with all different M values. The efficiency of these two AEs is around 90 % when $M = 2$ and reduced to 85 % and 73 % with $M = 10$ and 18, respectively. The other elements produced efficiency of more than 65 % when $M = 10$, and more than

TABLE 1. Maximum ECC over the entire frequency band with all M values in free space and with a user hand.

Number of AEs (M)	ECC	
	Free space	With hand
2	0.007	0.009
4	0.010	0.027
6	0.023	0.030
8	0.053	0.130
10	0.045	0.253
12	0.014	0.254
14	0.251	0.254
16	0.313	0.307
18	0.320	0.311

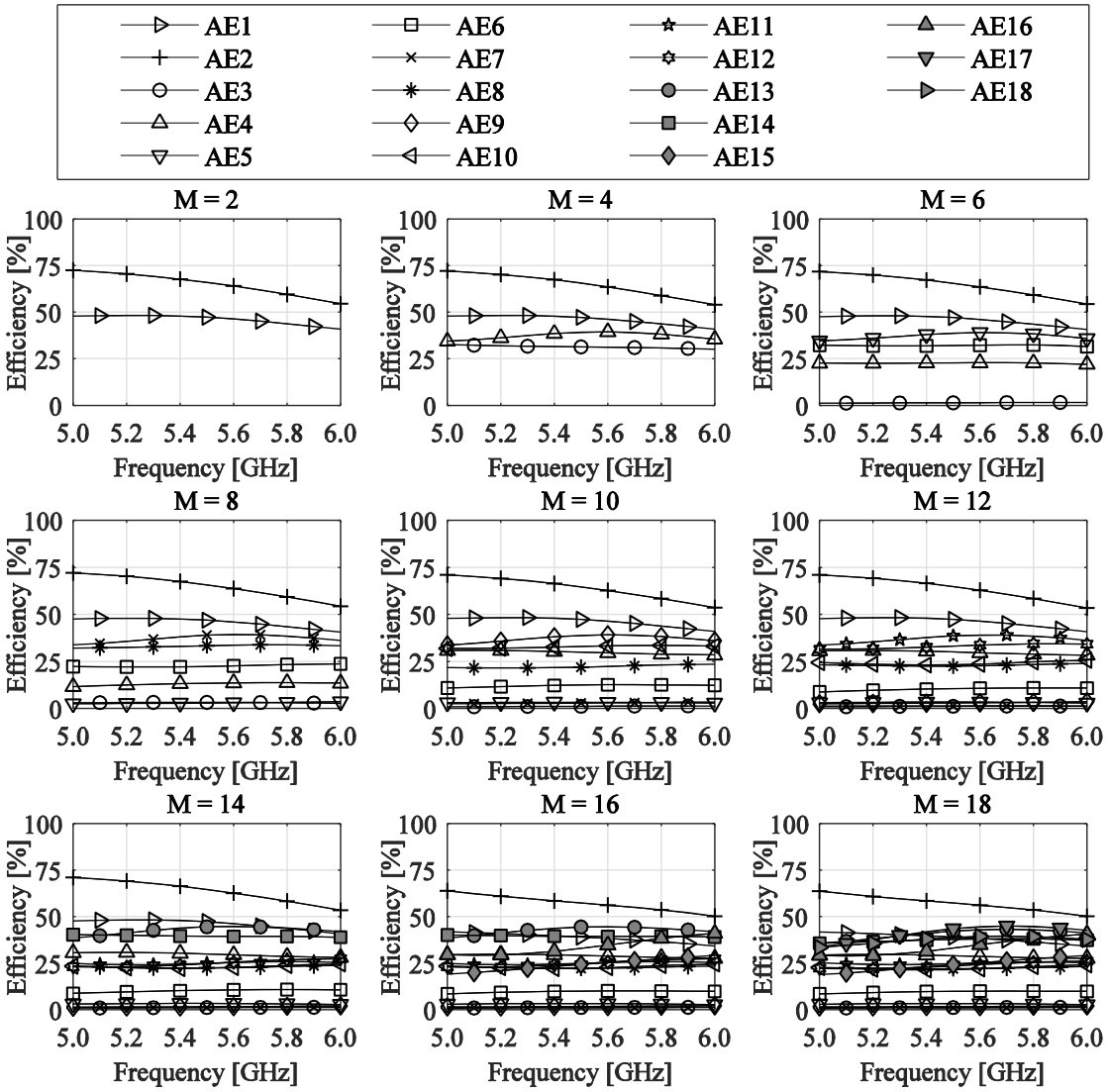

FIGURE 6. AEs efficiency of different of *M* with user hand.

50 % when $M = 18$. It is worth to note that AE15 and AE16 indicated the least efficiency when $M = 16$ and 18. The last two additional AEs, i.e. AE17 and AE18, exhibited at least 57 % of efficiencies when $M = 18$.

When evaluated in the proximity of the user hand, variation in the efficiency of each AE changes according to its interaction with the hand. AE2 is seen to produce the highest efficiency irrespective of the value of $\boldsymbol{M}$, which ranges from 73 % to 55% when $M = 2$. its level then reduces with increasing m to be between 64 % and 43 % when $M = 18$.

On the other hand, AE1 exhibited a more stable variation in efficiency level with frequency in comparison to AE2, which is about 50 % (when $M = 2$) and 40 % (when $M = 18$). It can be noticed that when $M = 6$ and above, several AEs suffered from complete signal blockage by the user hand, which resulted in their efficiencies of as low as 5 %. Several instances of such AEs are: i) AE3 (when $M = 6$); ii) AE3 and AE5 (when $M = 8$); iii) AE3, AE5, and AE7 (when $M = 10$), and; iv) AE3, AE5, AE7 and AE9 (when $M = 12$ *to*18). In addition to signal blockage, AE6 is also severely affected by user hand, with an efficiency of about 32 % when $M = 6$. This level then steadily decreased to around 10 % when M is 18. Meanwhile, other AEs exhibited efficiency levels of above around 25 % regardless of the values of M.

It is observed that the affected AEs are located on the vertical side of the chassis due to the obstruction by the fingers holding the terminal. On the other hand, the efficiency of the other elements located on the upper and lower horizontal sides of the chassis are degraded less. This efficiency degradation observation under the influence of user hand suggests that the strategic distribution of the AEs on the chassis and the correct choice of M can be used to improve the overall performance of the MIMO terminal.

B. MULTIPLEXING EFFICIENCY

Figure 7 shows the results of multiplexing efficiency (η_{mux}) in free space and with user hand effect. η_{mux} curves over the entire operating frequency band (from 5 to 6 GHz) are shown in Figure 7(a). In free space, η_{mux} is consistently above 90 % with $M = 2$ throughout the operating frequency. Besides that, η_{mux} also decreases with increasing M, resulting in the smallest free space η_{mux} ranging from 49 % to 65 % when $M = 16$ and 18. On the contrary, the level of η_{mux} with user hand with values of $M = 2$ and 4 is comparable with the free space η_{mux} values with $M = 16$ and 18. The minimum values of η_{mux} with user hand are as low as 13 % when M is 10 and higher (up to 18).

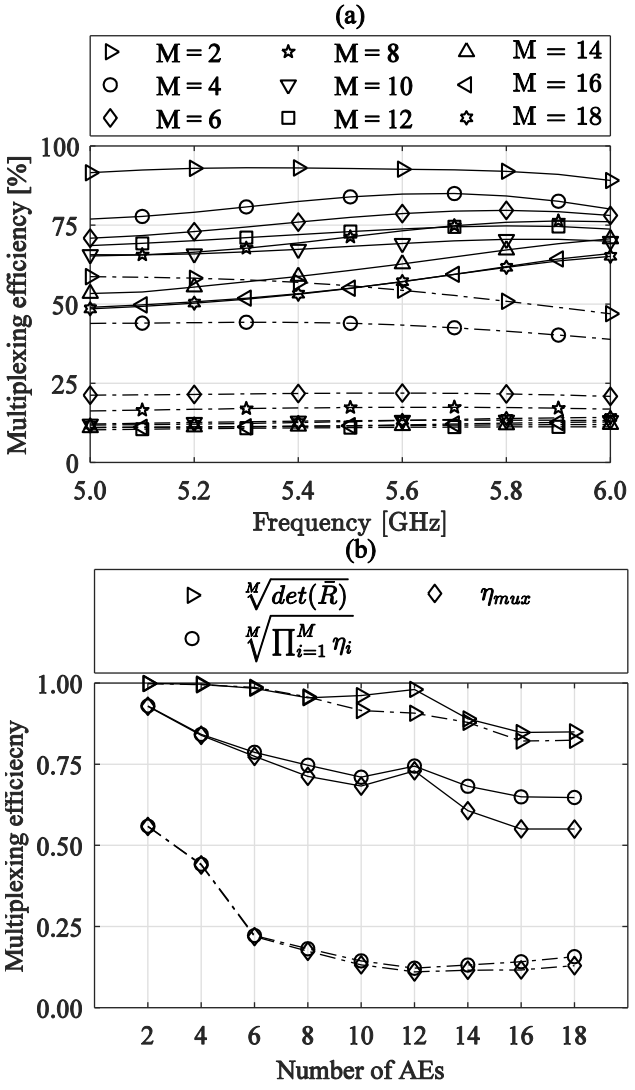

FIGURE 7. Multiplexing efficiency η_{mux} of the MIMO antennas with different numbers of AEs. (a) η_{mux} over the entire frequency band in free space (solid) and with user hand (dashed). (b) η_{mux} at center frequency 5.5 GHz in free space (solid) and with a user hand (dashed).

Figure 7(b) studies the η_{mux} (on a scale from 0 to 1) at the center operating frequency of 5.5 GHz for all M values in both cases of free space and with a user hand. In addition to that, the contribution from each term of the η_{mux} components in (13) i.e. $\sqrt[M]{\left(\prod_{i=1}^{M}\eta_i\right)}$ and $\sqrt[M]{det(\bar{R})}$ terms is studied. The user hand reduced η_{mux} by around 38 % when $M = 2$ and 4, and this reduction increased to 55 %. When $M = 6$, 8 and 10. The highest reduction is 62 % when $M = 12$. However, the reduction in η_{mux} is 45 % when M is 14, 16 and 18. This translates into average η_{mux} reduction of 49 % due to the effects of the user hand. The main factor contributing to the degradation of η_{mux} is seen to be originating from the $\sqrt[M]{\left(\prod_{i=1}^{M}\eta_i\right)}$ term. This is especially evident in the case with the user hand, which caused the efficiency of AEs decreased significantly. The contribution of the other term $\sqrt[M]{det(\bar{R})}$ in the degradation of η_{mux} is less significant in both free space and with user hand, as the value of this term is close to 1 with low values of M. The lowest values of the $\sqrt[M]{det(\bar{R})}$ term are seen when $M = 18$, with 0.85 and 0.82 in free space and with a user hand, respectively. Meanwhile, the value of $\sqrt[M]{\left(\prod_{i=1}^{M}\eta_i\right)}$ with the same number of AEs (i.e. 18) is 0.65 in free space and decreased to as low as 0.16 with the influence of the user hand. η_{mux} values at this number of AEs i.e. $M = 18$ are 0.55 and 0.13 in free space and with a user hand respectively. The analysis of the contribution from each term of the η_{mux} equation indicates that the capacity of the proposed MIMO system depends mainly on the efficiency of AEs. This also implies that the contribution from the low correlation between AEs is less significant. Based on these observations, priority in optimizing the performance of MIMO antennas in such cases should be given to enhance the efficiency of AEs. Such enhancement can be done by either designing more efficient AEs using suitable topologies and materials.

For brevity reasons, the next results, i.e. ergodic capacity and MRC performance, will be discussed at the center frequency of 5.5 GHz only.

C. ERGODIC CAPACITY

The next study performed in the context of capacity performance analysis is the ergodic capacity, which is calculated according to the channel model described in Section III.B. The number of random channels realization is 50,000M, (where M is the number of AEs) to ensure that averaging the capacities of the random channels realization converges to satisfactory accuracy. All results of the ergodic capacity are calculated at a SNR value of 20 dB

Figure 8(a) shows the ergodic capacity growth with M in both cases of free space and with a user hand, with the IID capacity plotted as a reference. In free space, the capacity increased from 11.06 to 49.50 and to 83.17 bit/s/Hz with $M = 2, 10$ and 18, respectively. However, these values are reduced under user hand influence to 9.86, 32.38 and 57.64 bit/s/Hz, respectively. It can be seen that the user hand reduces the ergodic capacity so severely that when $M = 18$,

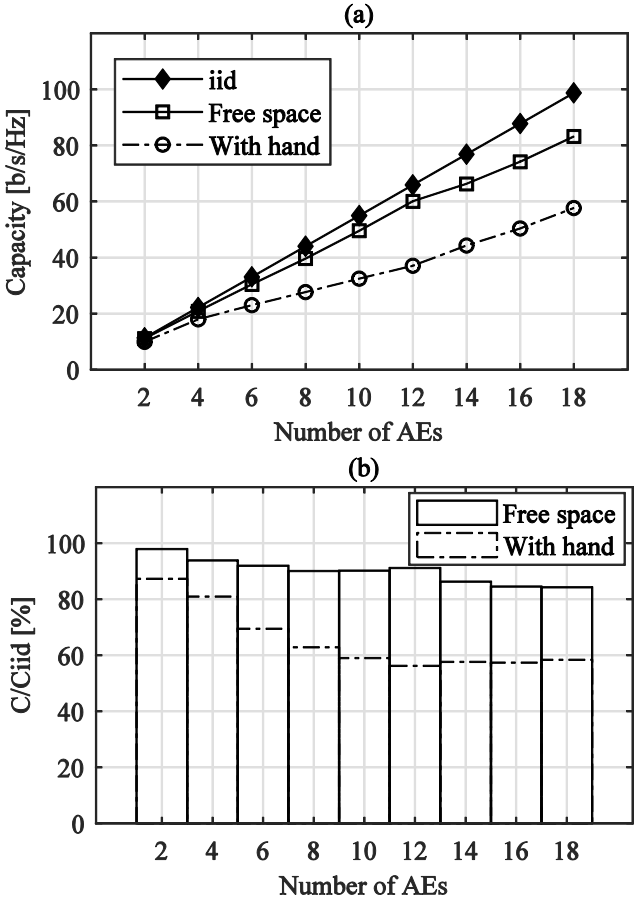

FIGURE 8. (a) Ergodic capacity in free space and with user hand. (b) The percentage from IID capacity achieved by MIMO antenna in free space and with a user hand.

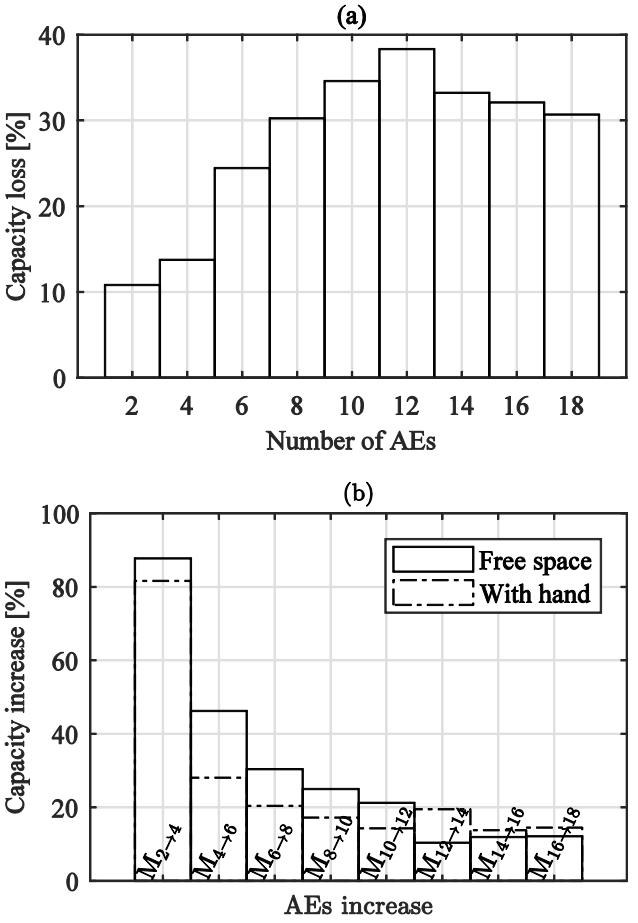

FIGURE 9. (a) Capacity loss due to user hand. (c) Capacity gained by increasing the number of AEs by two elements each time in free space and with user hand effect.

the resulting ergodic capacity is of the same level as seen in the free space for $M = 12$.

Next, the ergodic capacity of the designed MIMO antennas and the IID capacity are compared in Figure 8(b). The capacity (in percentage) achieved by the designed antennas is compared against the maximum possible capacity, i.e. IID capacity. In free space, the designed MIMO antenna achieved as high as 97 % of the IID capacity when $M = 2$, and this is reduced to 84 % when M reached 18. However, with user hand, the designed MIMO achieves 87 % from IID capacity with and $M = 2$, and this percentage consistently decreased down to 60 % when M is 8 and higher (up to 18).

Figure 9(a) shows the loss in ergodic capacity due to the user hand effect. Loss is calculated from the relation:

$$\text{Capacity loss} = \frac{c_{\text{free space}} - c_{\text{with user's hand}}}{c_{\text{free space}}} \times 100 \quad (16)$$

The loss due to user hand starts from 11 % with $M = 2$ and increases to a maximum value of 38 % when $M = 12$ before decreasing to around 31 % at $M = 18$.

Meanwhile, Figure 9(b) indicates the level of ergodic capacity obtained due to every increase of two AEs from i to j, which is denoted as $M_{i\to j}$. The percentage of capacity increase after each additional two AEs is integrated onto the mobile terminal (from i to j) is calculated as follows:

$$\text{Capacity increase} = \frac{c_j - c_i}{c_i} \times 100 \quad (17)$$

where c_i and c_j are the ergodic capacities with i and j number of AEs. Increasing M from 2 to 4 almost doubled the ergodic capacity to 88 % and 82 % in free space and with a user hand, respectively. Meanwhile, when M is increased from 4 to 6, the ergodic capacity increased by 46 % and 28 % in free space and with a user hand, respectively. The level of capacity improvement continues to decrease with the further increase of M, as more capacity accumulates in the denominator of (17). For instance, increasing M from 6 to 8 AEs in free space and with a user hand provided a capacity improvement of 30 % and 20 %, respectively, and increasing M from 8 to 10 AEs provided a capacity improvement of 25 % in free space and 17 % with a user hand. Each additional two AEs from 10 up to 18 improved the capacity by between 10 % and 21 %.

D. MRC TECHNIQUE

This section analyzes the results of the MRC technique, which MRC gain is illustrated in terms of CDF curves and

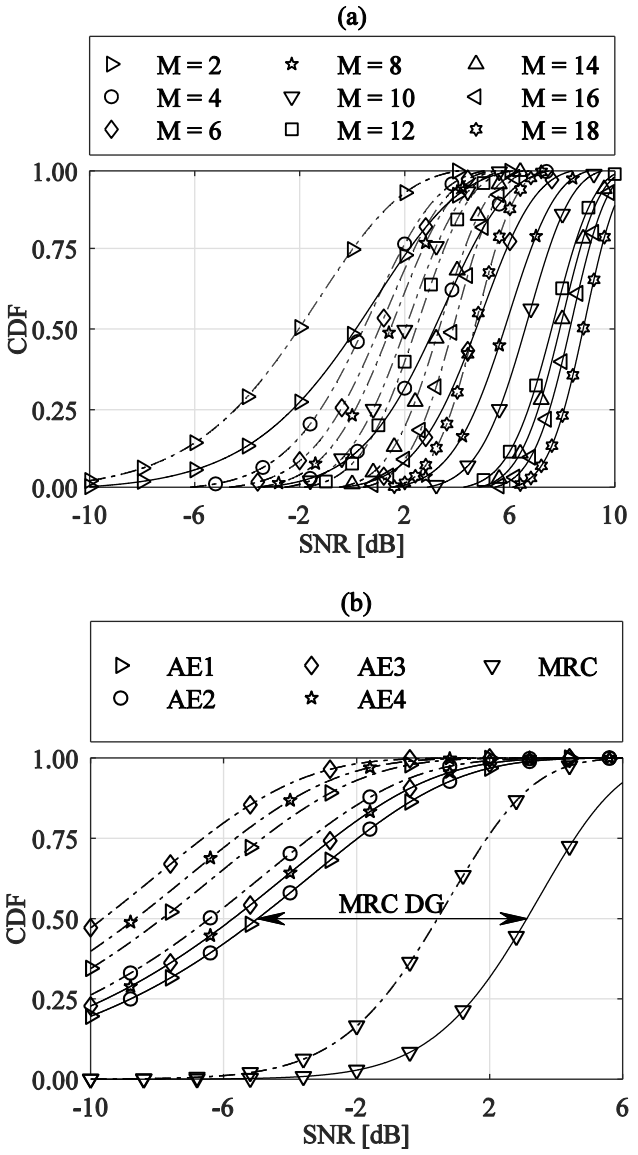

FIGURE 10. (a) CDF curves of the MRC gain with different M values in free space (solid) and with user hand (dashed). (b) CDF curves of the MRC gain and individual AEs of $M = 4$ in free space (solid) and with user hand (dashed).

is shown in Figure 10. The CDF curves of MRC gain for all M values in free space and with the effect of user hand are first illustrated in Figure 10(a). It is seen that the presence of the hand shifts the CDF curves to the lower values of normalized SNR. On the other hand, Figure 10(b) shows the CDF curves of the MRC gain of individual AEs, for the case of $M = 4$. These AEs indicated gain performance in the same order as their efficiencies, which were illustrated in Figure 5 and Figure 6. In free space, both AE1 and AE2 showed the same performance and the same goes for AE3 and AE4. However, with the influence of the user hand, the AEs behave differently, with AE3 most severely affected by the presence of the hand. Meanwhile, the same figure shows the concept of diversity gain, which is defined as the received signal gain of MRC relative to the highest gain among the individual AEs. Both gains corresponded to a certain CDF level, e.g. 0.1, 0.5 and 0.9.

Figure 11(a) shows the curves of the MRC gain and diversity gain (DG) extracted from CDF curves for all M values at the horizontal level of 0.5. The MRC gain in free space starts at 0.14 dB when $M = 2$, and increased to around 6.58 dB when $M = 10$. Slower increase in the MRC gain is obtained with an additional number of AEs after $M = 10$; an extra 2.22 dB is added when M reaches 18. On the contrary, signal absorption due to the user hand reduces MRC gain by around 2.44 dB with $M = 2$ and $M = 4$ in comparison to free space values. With additional AEs exceeding 4-elements, the average reduction in MRC gain is around 4.42 dB. The MRC DG in the same figure increased from 5.01 dB with $M = 2$ to around 11.86 dB with $M = 10$. A maximum value of 14.72 dB is achieved when M is 18. The increase of the MRC DG between $M = 2$ and $M = 10$ is around 6.81 dB. However, additional AEs exceeding ten and up to 18-elements increases the DG by only 2.86 dB. On the other hand, the user hand reduces the DG by around 0.69 dB, 1.24 dB and 2.33 dB with M of 2, 4 and 6, respectively, whereas this reduction increases for M values of higher

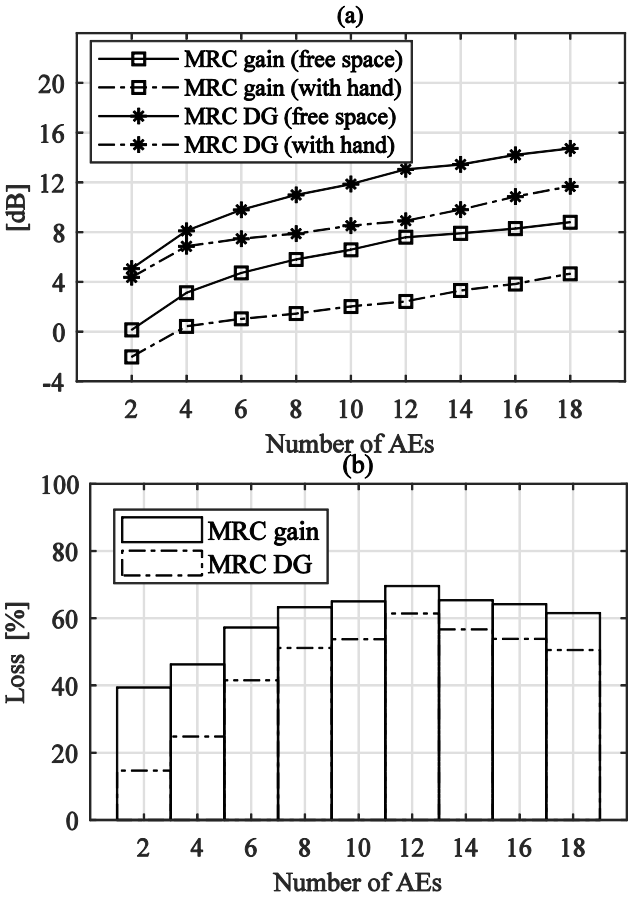

FIGURE 11. (a) MRC gain and DG calculated at a horizontal level of 50 % in free space and with a user hand. (b) Losses in MRC gain and DG at a horizontal level of 50 % caused by a user hand.

than 6, with an average value of 3.54 dB. The maximum reduction of the DG reduction is with $M = 12$ at 4.14 dB.

Next, the MRC gain and diversity gain are studied by including the losses caused by user hand. The loss is illustrated in Figure 11(b), and is calculated in the same way as in (16) while replacing capacity values with the linear MRC gain and DG. It can be observed that the loss behavior in this figure is similar to the trend shown in Figure 9(a) for the capacity loss, but with higher percentage values. This is mainly due to the dependence of the capacity and the MRC on the efficiency and MEG of the AEs, which are lowly related in a uniform environment, based on (5). The loss in MRC gain starts from 39 % with 2 AEs and it reaches its maximum 70 % with 12 AEs before getting reduced to 61 % when M is 18. The effect of the user hand on DG is less compared to the absolute gain, especially with low M values. DG loss is observed to be around 15 % when $M = 2$ and it reached maximum value of 61 % at $M = 12$, before being reduced to 51 % with the highest number of M (i.e. 18).

The final result in this section shows the increase in MRC gain and MRC DG with every additional two AEs. Equation (17) is used to calculate values in Figure 12 by replacing capacity values by linear MRC gain and MRC DG values. Both the MRC gain and MRC DG in this figure indicated the same trend, where the increase is around 100 % and 80 % in free space and with a user hand, respectively, upon the increase of the number of AEs from 2 to 4. The growth fluctuates between 8 % and 30 % upon each additional two AEs with M values of more than 6.

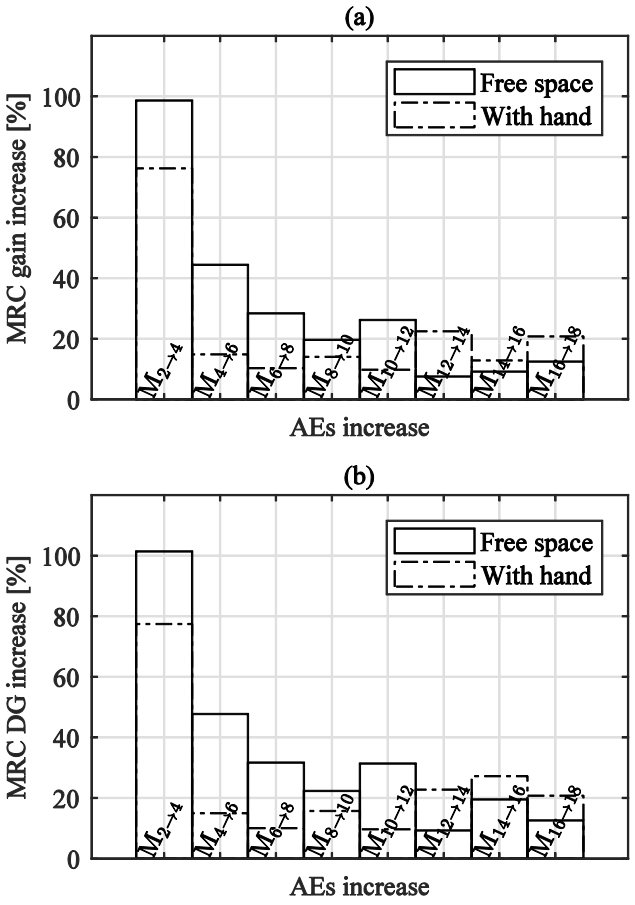

FIGURE 12. MRC gain increase (a) and MRC DG increase (b) with every additional 2-AEs in free space and with a user hand.

V. CONCLUSION

In this paper, the performance improvement of 5G MIMO antennas on a mobile terminal is studied with every two antenna element increase up to 18 elements, both in free space and the with a user hand when held in data mode. Free space evaluation of these antennas operating in the 5G frequency band ranging from 5 to 6 GHz indicated that an 18-element configuration on the same chassis operated with an efficiency of above 50 % and ECC of less than 0.32. In addition to that, the 18-element configuration in free space resulted in a capacity of about 84 % from the IID capacity. However, it is observed that the additional capacity obtained with every two additional antenna elements is between 10 and 20 % of the previous capacity after integrating ten elements onto the same chassis. This suggests that the amount of capacity improvement increases with the additional number of antenna elements up to a certain limit, and thus optimization on this parameter needs to be decided with care. On the contrary, the efficiency of antenna elements with the influence of the user hand dropped significantly. This is due to the complete blockage of certain elements by the hand and resulted in their efficiency degradation to below 5 %. It is generally observed that the capacity achieved with the influence of the user hand is about 60 % of the IID capacity when the number of elements is eight or higher. While a MIMO system on a mobile terminal operating in this band can be designed with up to 18 elements with satisfactory performance in free space. However, the performance is considerably degraded by the user hand. Moreover, the results also indicated that this degradation becomes more severe with the higher number of antenna elements. Thus, it can be concluded from the results that emphasis should be placed on strategies to mitigate the effects of user hand to obtain the optimized performance of MIMO mobile handsets. These include the design of antenna elements that are capable of operating with better coupling immunity when operating in the vicinity of a human hand, and more importantly, distributing these elements strategically on less obstructed locations throughout the chassis to reduce the possibility hand blockage. Finally, based on the results of this study a solution can be suggested to mitigate user's body effects and maintain a satisfactory performance under different scenarios of interactions with the user's body by providing sufficient extra antenna elements on the chassis, and the device periodically selects only elements operating with efficiencies over a certain threshold (need to be defined) and ignores elements below this threshold to save system resources. However, the total number of antenna elements on the chassis needs to be examined carefully under different usage scenarios (one-hand and two-hands scenarios) so that

the device will always be able to operate with the required number of antenna elements with acceptable efficiency

REFERENCES

[1] P. Varzakas, "Average channel capacity for Rayleigh fading spread spectrum MIMO systems," *Int. J. Commun. Syst.*, vol. 19, no. 10, pp. 1081–1087, Dec. 2006.

[2] D. Astély, E. Dahlman, A. Furuskär, Y. Jading, M. Lindström, and S. Parkvall, "LTE: The evolution of mobile broadband," *IEEE Commun. Mag.*, vol. 47, no. 4, pp. 44–51, Apr. 2009.

[3] W. Fan, X. Carreño, P. Kyösti, and J. Ø. Nielsen, "Over-the-air testing of Mimo-capable terminals," Ph.D. dissertation, Aalborg Univ., Aalborg, Denmark, Jun. 2015, pp. 38–46.

[4] B. Rohani, K. Takahashi, H. Arai, Y. Kimura, and T. Ihara, "Improving channel capacity in indoor 4 × 4 MIMO base station utilizing small bidirectional antenna," *IEEE Trans. Antennas Propag.*, vol. 66, no. 1, pp. 393–400, Jan. 2018.

[5] B. Yanakiev, J. Ø. Nielsen, M. Christensen, and G. F. Pedersen, "On small terminal antenna correlation and impact on MIMO channel capacity," *IEEE Trans. Antennas Propag.*, vol. 60, no. 2, pp. 689–699, Feb. 2012.

[6] D. Gesbert, M. Shafi, D.-S. Shiu, P. Smith, and A. Naguib, "From theory to practice: An overview of MIMO space-time coded wireless systems," *IEEE J. Sel. Areas Commun.*, vol. 21, no. 3, pp. 281–302, Apr. 2003.

[7] F. Harrysson, A. Derneryd, and F. Tufvesson, "Evaluation of user hand and body impact on multiple antenna handset performance," in *Proc. IEEE Antennas Propag. Soc. Int. Symp.*, Jul. 2010, pp. 1–4.

[8] S. S. Zhekov, A. Tatomirescu, E. Foroozanfard, and G. F. Pedersen, "Experimental investigation on the effect of user's hand proximity on a compact ultrawideband MIMO antenna array," *IET Microw., Antennas Propag.*, vol. 10, no. 13, pp. 1402–1410, Oct. 2016.

[9] R. Khan, A. A. Al-Hadi, and P. J. Soh, "Recent advancements in user effect mitigation for mobile terminal antennas: A review," *IEEE Trans. Electromagn. Compat.*, vol. 61, no. 1, pp. 279–287, Feb. 2019.

[10] J. Holopainen, O. KivekÄs, J. Ilvonen, R. Valkonen, C. Icheln, and P. Vainikainen, "Effect of the user's hands on the operation of lower UHF-band mobile terminal antennas: Focus on digital television receiver," *IEEE Trans. Electromagn. Compat.*, vol. 53, no. 3, pp. 831–841, Aug. 2011.

[11] Q. H. Abbasi, H. El Sallabi, E. Serpedin, K. Qaraqe, A. Alomainy, and Y. Hao, "Ellipticity statistics of ultra wideband MIMO channels for body centric wireless communication," in *Proc. 10th Eur. Conf. Antennas Propag. (EuCAP)*, Apr. 2016, pp. 1–4.

[12] J. Helander, K. Zhao, Z. Ying, and D. Sjoberg, "Performance analysis of millimeter-wave phased array antennas in cellular handsets," *IEEE Antennas Wireless Propag. Lett.*, vol. 15, pp. 504–507, 2016.

[13] K. Zhao, J. Helander, D. Sjoberg, S. He, T. Bolin, and Z. Ying, "User body effect on phased array in user equipment for the 5G mmWave communication system," *IEEE Antennas Wireless Propag. Lett.*, vol. 16, pp. 864–867, 2017.

[14] S. Zhang, X. Chen, I. Syrytsin, and G. F. Pedersen, "A planar switchable 3-D-coverage phased array antenna and its user effects for 28-GHz mobile terminal applications," *IEEE Trans. Antennas Propag.*, vol. 65, no. 12, pp. 6413–6421, Dec. 2017.

[15] J. G. Andrews, S. Buzzi, W. Choi, S. V. Hanly, A. Lozano, A. C. K. Soong, and J. C. Zhang, "What will 5G be?" *IEEE J. Sel. Areas Commun.*, vol. 32, no. 6, pp. 1065–1082, Jun. 2014.

[16] M. S. Sharawi, M. Ikram, and A. Shamim, "A two concentric slot loop based connected array MIMO antenna system for 4G/5G terminals," *IEEE Trans. Antennas Propag.*, vol. 65, no. 12, pp. 6679–6686, Dec. 2017.

[17] M.-Y. Li, Y.-L. Ban, Z.-Q. Xu, G. Wu, C.-Y.-D. Sim, K. Kang, and Z.-F. Yu, "Eight-port orthogonally dual-polarized antenna array for 5G smartphone applications," *IEEE Trans. Antennas Propag.*, vol. 64, no. 9, pp. 3820–3830, Sep. 2016.

[18] A. A. Al-Hadi, J. Ilvonen, R. Valkonen, and V. Viikari, "Eight-element antenna array for diversity and MIMO mobile terminal in LTE 3500 MHz band," *Microw. Opt. Technol. Lett.*, vol. 56, no. 6, pp. 1323–1327, Jun. 2014.

[19] Y.-L. Ban, C. Li, C.-Y.-D. Sim, G. Wu, and K.-L. Wong, "4G/5G multiple antennas for future multi-mode smartphone applications," *IEEE Access*, vol. 4, pp. 2981–2988, 2016.

[20] X. Shi, M. Zhang, S. Xu, D. Liu, H. Wen, and J. Wang, "Dual-band 8-element MIMO antenna with short neutral line for 5G mobile handset," in *Proc. 11th Eur. Conf. Antennas Propag. (EUCAP)*, Mar. 2017, pp. 3140–3142.

[21] W. Jiang, B. Liu, Y. Cui, and W. Hu, "High-isolation eight-element MIMO array for 5G smartphone applications," *IEEE Access*, vol. 7, pp. 34104–34112, 2019.

[22] M.-Y. Li, Z.-Q. Xu, Y.-L. Ban, C.-Y.-D. Sim, and Z.-F. Yu, "Eight-port orthogonally dual-polarised MIMO antennas using loop structures for 5G smartphone," *IET Microw., Antennas Propag.*, vol. 11, no. 12, pp. 1810–1816, Sep. 2017.

[23] K. Wong and J. Lu, "3.6-GHz 10-antenna array for MIMO operation in the smartphone," *Microw. Opt. Technol. Lett.*, vol. 57, no. 7, pp. 1699–1704, 2015.

[24] J.-Y. Deng, J. Yao, D.-Q. Sun, and L.-X. Guo, "Ten-element MIMO antenna for 5G terminals," *Microw. Opt. Technol. Lett.*, vol. 60, no. 12, pp. 3045–3049, Dec. 2018.

[25] M.-Y. Li, Y.-L. Ban, Z.-Q. Xu, J. Guo, and Z.-F. Yu, "Tri-polarized 12-antenna MIMO array for future 5G smartphone applications," *IEEE Access*, vol. 6, pp. 6160–6170, 2018.

[26] Y. Li, C.-Y.-D. Sim, Y. Luo, and G. Yang, "12-port 5G massive MIMO antenna array in sub-6 GHz mobile handset for LTE bands 42/43/46 applications," *IEEE Access*, vol. 6, pp. 344–354, 2018.

[27] K.-L. Wong, J.-Y. Lu, L.-Y. Chen, W.-Y. Li, and Y.-L. Ban, "8-antenna and 16-antenna arrays using the quad-antenna linear array as a building block for the 3.5-GHz LTE MIMO operation in the smartphone," *Microw. Opt. Technol. Lett.*, vol. 58, no. 1, pp. 174–181, Jan. 2016.

[28] H. Xu, H. Wang, S. Gao, H. Zhou, Y. Huang, Q. Xu, and Y. Cheng, "A compact and low-profile loop antenna with six resonant modes for LTE smartphone," *IEEE Trans. Antennas Propag.*, vol. 64, no. 9, pp. 3743–3751, Sep. 2016.

[29] C. Di Paola, I. Syrytsin, S. Zhang, and G. Pedersen, "Investigation of user effects on mobile phased antenna array from 5 to 6 GHz," in *Proc. 12th Eur. Conf. Antennas Propag. (EuCAP)*, 2018.

[30] N. O. Parchin, H. J. Basherlou, Y. I. A. Al-Yasir, A. Ullah, R. A. Abd-Alhameed, and J. M. Noras, "Multi-band MIMO antenna design with user-impact investigation for 4G and 5G mobile terminals," *Sensors*, vol. 19, no. 3, p. 456, Jan. 2019.

[31] C.-Y.-D. Sim, H.-Y. Liu, and C.-J. Huang, "Wideband MIMO antenna array design for future mobile devices operating in the 5G NR frequency bands n77/n78/n79 and LTE band 46," *IEEE Antennas Wireless Propag. Lett.*, vol. 19, no. 1, pp. 74–78, Jan. 2020.

[32] J. Li, X. Zhang, Z. Wang, X. Chen, J. Chen, Y. Li, and A. Zhang, "Dual-band eight-antenna array design for MIMO applications in 5G mobile terminals," *IEEE Access*, vol. 7, pp. 71636–71644, 2019.

[33] Z. Ying, "Antennas in cellular phones for mobile communications," *Proc. IEEE*, vol. 100, no. 7, pp. 2286–2296, Jul. 2012.

[34] M. S. Sharawi, "Current misuses and future prospects for printed multiple-input, multiple-output antenna systems," *IEEE Antennas Propag. Mag.*, vol. 59, no. 2, pp. 162–170, Apr. 2017.

[35] D. Sun and C. Wei, "Analysis and design of 4 × 4 MIMO-antenna systems in mobile phone," *J. Comput. Commun.*, vol. 4, no. 2, p. 26, 2016.

[36] J.-M. Lee, K.-B. Kim, H.-K. Ryu, and J.-M. Woo, "A compact ultrawideband MIMO antenna with WLAN band-rejected operation for mobile devices," *IEEE Antennas Wireless Propag. Lett.*, vol. 11, pp. 990–993, 2012.

[37] M. S. Sharawi, "Printed multi-band MIMO antenna systems and their performance metrics [wireless corner]," *IEEE Antennas Propag. Mag.*, vol. 55, no. 5, pp. 218–232, Oct. 2013.

[38] M. S. Sharawi, A. T. Hassan, and M. U. Khan, "Correlation coefficient calculations for MIMO antenna systems: A comparative study," *Int. J. Microw. Wireless Technol.*, vol. 9, no. 10, pp. 1991–2004, Dec. 2017.

[39] C. A. Balanis, *Modern Antenna Handbook*. Hoboken, NJ, USA: Wiley, 2011.

[40] A. A. Glazunov, A. Molisch, and F. Tufvesson, "Mean effective gain of antennas in a wireless channel," *IET Microw. Antennas Propag.*, vol. 3, no. 2, pp. 214–227, 2009.

[41] K. Zhao, E. Bengtsson, Z. Ying, and S. He, "Multiplexing efficiency of high order MIMO in mobile terminal in different propagation scenarios," in *Proc. 10th Eur. Conf. Antennas Propag. (EuCAP)*, Apr. 2016, pp. 1–4.

[42] R. Tian, B. K. Lau, and Z. Ying, "Multiplexing efficiency of MIMO antennas with user effects," in *Proc. IEEE Int. Symp. Antennas Propag.*, Jul. 2012, pp. 1–2.
[43] I. Vasilev, V. Plicanic, and B. K. Lau, "Impact of antenna design on MIMO performance for compact terminals with adaptive impedance matching," *IEEE Trans. Antennas Propag.*, vol. 64, no. 4, pp. 1454–1465, Apr. 2016.
[44] X. Chen and S. Zhang, "Multiplexing efficiency for MIMO antenna-channel impairment characterisation in realistic multipath environments," *IET Microw., Antennas Propag.*, vol. 11, no. 4, pp. 524–528, Mar. 2017.
[45] R. Tian, B. K. Lau, and Z. Ying, "Multiplexing efficiency of MIMO antennas," *IEEE Antennas Wireless Propag. Lett.*, vol. 10, pp. 183–186, 2011.
[46] X. Chen, "Antenna correlation and its impact on multi-antenna system," *Prog. Electromagn. Res.*, vol. 62, pp. 241–253, 2015.
[47] S. P. Jadhav and V. S. Hendre, "Performance of maximum ratio combining (MRC) MIMO systems for Rayleigh fading channel," *Int. J. Sci. Res. Publ.*, vol. 3, no. 2, pp. 1–4, 2013.
[48] V. Papamichael, M. Karaboikis, C. Soras, and V. Makios, "Diversity and MIMO performance evaluation of common phase center multi element antenna systems," *Radioengineering*, vol. 17, no. 2, p. 33, 2008.

AHMED MOHAMED ELSHIRKASI received the M.Sc. degree in communication engineering from International Islamic University Malaysia (IIUM), in 2015. He is currently pursuing the Ph.D. degree with Universiti Malaysia Perlis (UniMAP). His current research interests include the performance evaluation of multielement antennas, mobile terminal antennas and their user interactions, and wireless propagation.

AZREMI ABDULLAH AL-HADI (Senior Member, IEEE) was born in Michigan, USA, in August 26. He received the M.Sc. degree in communication engineering from Birmingham University, U.K., in 2004, and the D.Sc. degree in technology from Aalto University, Finland, in 2013.

His current research interests include design and performance evaluation of multielement antennas, mobile terminal antennas and their user interactions, and wireless propagation. He is currently working as an Associate Professor and holds a position as the Dean of the School of Computer and Communication Engineering, Universiti Malaysia Perlis (UniMAP), where he has been with the School of Computer and Communication Engineering, since 2002.

Dr. Al-Hadi is active in volunteering work with the IEEE Malaysia Section, acting as the Vice Chair of the IEEE Antenna Propagation/Microwave Theory Techniques/Electromagnetic Compatibility (AP/MTT/EMC) Malaysia Chapter, and the Counselor of the IEEE UniMAP Student Branch. He is a Chartered Engineer of the Institution of Engineering and Technology (IET), U.K., a member of the Board of Engineers Malaysia (BEM), Malaysia, and a Graduate Technologist of the Malaysia Board of Technologist (MBOT), Malaysia. He was a recipient of the Best Student Paper Award presented at the Fifth Loughborough Antennas and Propagation Conference (LAPC 2009) and the CST University Publication Award, in 2011.

PING JACK SOH (Senior Member, IEEE) was born in Sabah, Malaysia. He received the B.Eng. and M.Eng. degrees from Universiti Teknologi Malaysia, and the Ph.D. degree from the ESAT-TELEMIC Research Division, KU Leuven, Belgium.

He is currently an Associate Professor with the School of Computer and Communication Engineering, Universiti Malaysia Perlis (UniMAP), and a Research Affiliate with KU Leuven. From 2002 to 2004, he was a Test Engineer with Venture Corporation. In 2005, he joined Motorola Solutions Malaysia, as a Research and Development Engineer. Since 2006, he has been a Lecturer with UniMAP before pursuing the Ph.D. degree with the ESAT-TELEMIC Research Division, KU Leuven, as a Research Assistant, from 2009 to 2013, and then a Postdoctoral Fellow, from 2013 to 2014. He studies actively in his areas of interest such as wearable and flexible antennas/metasurfaces, on-body communication, electromagnetic safety and absorption, and wireless and radar techniques for healthcare applications. He was a recipient of the IEEE AP-S Doctoral Research Award, in 2012, the IEEE MTT-S Graduate Fellowship for Medical Applications, in 2013, and the URSI Young Scientist Award, in 2015. He was also the Second Place Winner of the IEEE Presidents' Change the World Competition, in 2013. He is a registered Chartered Engineer of the U.K. Engineering Council, a registered Professional Technologist with the Malaysia Board of Technologist (MBOT), and a member of the IET and URSI. He also serves on the IEEE MTT-S Education Committee and the IEEE MTT-S Meetings and Symposia (M&S) Committee.

MOHD FAIS MANSOR (Member, IEEE) was born in Selangor, Malaysia, in 1981. He received the B.Eng. degree in computer and communication from Universiti Kebangsaan Malaysia (UKM), in 2005, and the Ph.D. degree in antenna and propagation from the University of Surrey, U.K., in 2012. He has been with UKM, since 2005, where he is currently a Senior Lecturer with the Centre of Advanced Electronic and Communication Engineering and the Coordinator of UKM International Office at UDE. He was a Visiting Researcher with the Institute of Digital Signal Processing, University of Duisburg–Essen (UDE), Germany, from August 2017 to July 2018, in MARIE project sponsored by the German Research Foundation. Since 2008, he has been involved in MIMO antenna design and evaluation with a special focus on satellite MIMO system. His main areas of research are MIMO antenna design and evaluation, reconfigurable antennas, and mm-Wave antennas and RF circuits.

RIZWAN KHAN was born in Abbottabad, Pakistan, in 1990. He received the M.S. degree in electrical engineering from the COMSATS Institute of Information Technology, Abbottabad, in 2015, and the D.Sc. degree in communication engineering from Universiti Malaysia Perlis (UniMAP), in 2018. From 2015 to 2016, he has served as a Research Associate with the Department of Electrical Engineering, COMSATS Institute of Information Technology. He has published several impact factor journals, and national and international conference papers. He is currently working as a RF Engineer with Laird Technologies (M) Sdn Bhd, Penang, Malaysia. He also involves in research with the Advanced Communication Engineering (ACE) Center of Excellence, UniMAP, Malaysia. His research interests include mobile terminal antennas and their user interactions, MIMO antennas, dielectric resonator antennas, metamaterial, electrically small antennas, and reconfigurable antennas.

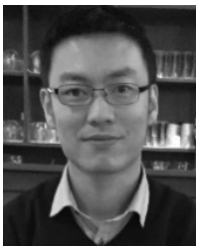

XIAOMING CHEN received the B.Sc. degree in electrical engineering from Northwestern Polytechnical University, Xi'an, China, in 2006, and the M.Sc. and Ph.D. degrees in electrical engineering from the Chalmers University of Technology, Gothenburg, Sweden, in 2007 and 2012, respectively.

From 2013 to 2014, he was a Postdoctoral Researcher with the same University. From 2014 to 2017, he was with Qamcom Research and Technology AB, Gothenburg, where he was involved in the EU H2020 5GPPP mmMAGIC Project (working on 5G millimeter-Wave wireless access techniques). Since 2017, he has been a Professor with Xi'an Jiaotong University, Xi'an. His research areas include 5G multiantenna techniques, over-the-air (OTA) testing, reverberation chambers, and hardware impairments and mitigation. He has coauthored one book, one book chapter, more than 60 journal articles, and over 60 conference papers on his research topics. He received the International Union of Radio Science (URSI) Young Scientist Awards, in 2017 and 2018. He serves as an Associate Editor (AE) for the journal of *IEEE Antennas and Wireless Propagation Letters*. He received the outstanding AE awards, in 2018 and 2019. He was also a Guest Editor of the Special Issue on Metrology for 5G Technologies of the journal of *IET Microwaves, Antennas & Propagation*.

PRAYOOT AKKARAEKTHALIN (Member, IEEE) received the B.Eng. and M.Eng. degrees in electrical engineering from the King Mongkut's University of Technology North Bangkok (KMUTNB), Bangkok, Thailand, in 1986 and 1990, respectively, and the Ph.D. degree from the University of Delaware, Newark, DE, USA, in 1998. From 1986 to 1988, he was a Research and Development Engineer with Microtek Company, Ltd., Thailand. In 1988, he joined the Department of Electrical Engineering, KMUTNB. He has authored or coauthored over 40 international journals, more than 200 conference papers, and four books/book chapters. He is currently the Leader of TRF Senior Research Scholar Project of Innovative Sensor Technology for Thailand Development granted by the Thailand Research Fund, Thailand. His current research interests include RF/microwave circuits, wideband and multiband antennas, telecommunications, and sensor systems. He is a member of the IEICE, Japan, ECTI, and EEAAT Associations, Thailand. He was the Chairman of the IEEE MTT/AP/ED Thailand Joint Chapter, from 2007 to 2010, and the Vice President and President of the ECTI Association, Thailand, from 2012 to 2013 and from 2014 to 2015, respectively. He was the Editor-in-Chief of the *ECTI Transactions*, from 2011 to 2013.